AEDC-TR-78-32

OPTICAL IN SITU VERSUS PROBE MEASUREMENTS OF NITRIC OXIDE CONCENTRATION AS A FUNCTION OF AXIAL POSITION IN A COMBUSTOR EXHAUST

J. D. Few, R. J. Bryson, and H. S. Lowry III
ARO, Inc., a Sverdrup Corporation Company

ENGINE TEST FACILITY
ARNOLD ENGINEERING DEVELOPMENT CENTER
AIR FORCE SYSTEMS COMMAND
ARNOLD AIR FORCE STATION, TENNESSEE 37389

March 1979

Final Report for Period 21 July — 27 August 1977

Prepared for

DET 1, HQ ARMAMENT DEVELOPMENT AND TEST CENTER/ECC
TYNDALL AIR FORCE BASE, FLORIDA 32401

NOTICES
When U. S. Government drawings, specifications, or other data are used for any purpose other than a definitely related Government procurement operation, the Government thereby incurs no responsibility nor any obligation whatsoever, and the fact that the Government may have formulated, furnished, or in any way supplied the said drawings, specifications, or other data, is not to be regarded by implication or otherwise, or in any manner licensing the holder or any other person or corporation, or conveying any rights or permission to manufacture, use, or sell any patented invention that may in any way be related thereto.
Qualified users may obtain copies of this report from the Defense Documentation Center.
References to named commerical products in this report are not to be considered in any sense as an indorsement of the product by the United States Air Force or the Government.

This report has been reviewed by the Information Office (OI) and is releasable to the National Technical Information Service (NTIS). At NTIS, it will be available to the general public, including foreign nations.

APPROVAL STATEMENT

This report has been reviewed and approved.

Eules L. Hively

EULES L. HIVELY
Project Manager, Research Division
Directorate of Test Engineering

Approved for publication:

FOR THE COMMANDER

Robert W. Crossley

ROBERT W. CROSSLEY, Lt Colonel, USAF
Acting Director of Test Engineering
Deputy for Operations

REPORT DOCUMENTATION PAGE		READ INSTRUCTIONS BEFORE COMPLETING FORM
1 REPORT NUMBER AEDC-TR-78-32	2 GOVT ACCESSION NO.	3. RECIPIENT'S CATALOG NUMBER
4. TITLE (and Subtitle) OPTICAL IN SITU VERSUS PROBE MEASUREMENTS OF NITRIC OXIDE CONCENTRATION AS A FUNCTION OF AXIAL POSITION IN A COMBUSTOR EXHAUST		5 TYPE OF REPORT & PERIOD COVERED Final Report, 21 July - 27 August 1977 6 PERFORMING ORG. REPORT NUMBER
7. AUTHOR(s) J. D. Few, R. J. Bryson, and H. S. Lowry III, ARO, Inc.		8 CONTRACT OR GRANT NUMBER(s)
9 PERFORMING ORGANIZATION NAME AND ADDRESS Arnold Engineering Development Center Air Force Systems Command Arnold Air Force Station, TN 37389		10. PROGRAM ELEMENT, PROJECT, TASK AREA & WORK UNIT NUMBERS Program Element 62601F
11. CONTROLLING OFFICE NAME AND ADDRESS Det 1, HQ Armament Development and Test Center/ECC, Tyndall Air Force Base, FL 32401		12. REPORT DATE March 1979 13 NUMBER OF PAGES 34
14. MONITORING AGENCY NAME & ADDRESS(if different from Controlling Office)		15. SECURITY CLASS. (of this report) UNCLASSIFIED 15a. DECLASSIFICATION/DOWNGRADING SCHEDULE N/A

16. DISTRIBUTION STATEMENT (of this Report)
Approved for public release; distribution unlimited.

17. DISTRIBUTION STATEMENT (of the abstract entered in Block 20, if different from Report)

18. SUPPLEMENTARY NOTES
Available in DDC.

19 KEY WORDS (Continue on reverse side if necessary and identify by block number)

emission	absorption (physical)
jet engines	optics
exhaust gases	
probes	
samplers	

20. ABSTRACT (Continue on reverse side if necessary and identify by block number)
Nitric oxide (NO) concentration was measured at three axial stations (6.5, 12, and 25 nozzle diameters downstream of a combustor nozzle exit) in a jet engine combustor exhaust by a gas-sampling probe in conjunction with conventional gas analyzers and an optical resonance absorption technique. The gas analyzer system permitted measurements of NO, NO_x, CO, CO_2, and C_xH_y (total hydrocarbons) whereas the optical absorption technique

DD FORM 1 JAN 73 1473 EDITION OF 1 NOV 65 IS OBSOLETE

20. ABSTRACT (CONTINUED)

permitted measurement of NO only. The combustor was exhausted into a test cell of slightly less than atmospheric pressure and was operated at an inlet air temperature of 589°K, a total pressure of 344.3 kPa, and a fuel-to-air ratio (f/a) of 0.02. A multiprobe rake was used to acquire emissions, total pressure and temperature, and static pressure data at the measurement stations. The measurements of total pressure, total temperature, and measured static pressure were used to determine static temperature and pressure profiles at each measurement station, which are required for determining NO concentration by the optical absorption technique. The optically measured NO concentrations were consistently higher than the probe-measured NO concentrations by factors of two to four. NO concentration measurements using a probe system, which maintained a low pressure (41.3 kPa) from the entrance of a quartz sample probe through the transfer line and reaction chamber of a chemiluminescence analyzer, were compared to results obtained using an orifice-type probe at 12 nozzle diameters downstream. No measurable differences were found. The possibility that the differences which exist between NO concentration measurements made by probe sampling and those made by an optical in situ technique may be temperature dependent prompted a study in which the entrance region of a sample probe was simulated to determine the effects of temperature on calibration gases introduced into the probe. A mixture of calibration gases was introduced (NO, CO, CO_2, N_2, and CH_4) in the presence of a small percentage of hydrogen gas, and it was found that the NO concentration level was reduced at elevated temperatures (>617°K). At the same time the NO level was reduced, it was found that the CO level was increased. Further results indicate that the above-mentioned reactions are inhibited by the addition of oxygen to the mixture.

AFSC
Arnold AFB Tenn

PREFACE

The work reported herein was conducted by the Arnold Engineering Development Center (AEDC), Air Force Systems Command (AFSC), at the request of Det 1, HQ Armament Development and Test Center/ECC, Tyndall Air Force Base, Florida. The results of the research were obtained by ARO, Inc., AEDC Division (a Sverdrup Corporation Company), operating contractor for the AEDC, AFSC, Arnold Air Force Station, Tennessee under Project Numbers R34P-F5A and R32P-C6A. The data analysis was completed on September 23, 1977, and the manuscript was submitted for publication on April 25, 1978.

The authors wish to express their sincere appreciation to Dr. R. J. Schulz and Dr. C. E. Peters, ARO, Inc., for the solution to a recirculation problem which existed in the R-2C-1 research facility in the early stages of operation. In addition, the assistance provided by Mr. L. F. Smith, ARO, Inc., from system buildup through data reduction is gratefully acknowledged.

CONTENTS

ILLUSTRATIONS

Figure | Page

TABLES

1.0 INTRODUCTION

The differences between measured values of nitric oxide (NO) concentration obtained by gas sampling and in situ optical techniques in combustor gas flows have been established (Ref. 1). Previous investigations have indicated the possibility that the differences in the measurement results obtained by the two techniques may be dependent upon the exhaust gas temperature (Ref. 2). The research reported here was conducted to investigate further this possible temperature dependence of the two types of measurements in a combustor facility.

Emissions measurements in the exhaust of an AVCO-Lycoming combustor located in Research Cell R-2C-1 in the AEDC Engine Test Facility (ETF) are presented at three axial locations corresponding to 6.5, 12, and 25 nozzle diameters downstream of the combustor nozzle exit plane using both gas-sampling probes and an optical absorption technique. Optical in situ data were obtained for NO only, whereas sample probe data were obtained for NO, NO_x, CO, CO_2, and C_xH_y (total hydrocarbons). Gas dynamic data were obtained at each of the stations to define static temperature and pressure, which are required for the determination of the NO concentration from the optical absorption measurements.

Measured values of NO concentration using the probe technique are compared to the NO concentration values obtained using the optical technique on a point by point basis along the radius at each measurement station. These comparisons show that the optical technique consistently gives higher values for NO concentration in the exhaust than does the probe-sampling technique. It was found that the centerline ratio of optical to probe measured NO concentration varied from approximately four at the 6.5 nozzle diameter station to about two at the 25 nozzle diameter station. The centerline static temperature at these same two stations decreased from 970 to 470°K.

Work done in measuring NO concentrations in laboratory experiments (Ref. 3) led to the possibility that the accuracy of NO concentration measurements made by a chemiluminescence-type gas analyzer in a combustor exhaust could be improved by lowering the pressure in the gas sample at the entrance to the sample probe to a level below about 1.33 kPa. This pressure level must also be maintained in the gas sample until it has been through the analysis instrument. A quartz gas sample probe and chemiluminescence NO analyzer system designed to operate under these low-pressure conditions was used to make NO concentration measurements at one axial location in the combustor exhaust. NO concentrations determined with this system were compared to those obtained at the same location with a conventional, orifice-type probe and analyzer system and were found to be equal.

The possibility that the differences that exist between NO concentration measurements made by probe sampling and by an in situ technique may be temperature dependent prompted a study in which the entrance region of a sampling probe was heated to determine the effects of temperature on calibration gases introduced into the probe. It was found that the NO concentration level in some gas samples could be reduced at elevated temperatures (above about 617°K) in the presence of H_2 gas. At the same time that the NO level was reduced, it was found that the CO level increased if CO_2 was present along with the H_2. The results show the same trends as results obtained by Benson and Samuelson (Ref. 4) in a similar study. The present results yield the additional information that both the above reactions are inhibited by the addition of O_2 to the gas sample.

2.0 DESCRIPTION OF APPARATUS

The experimental apparatus described in this report was installed in AEDC/ETF test cell R-2C-1. The apparatus was designed to facilitate the measurement of turbine combustor exhaust species concentrations by two independent measurement techniques. The test installation included a turbine engine combustor and associated operational equipment, the test section, a resonance spectral absorption system, and a conventional gas analysis system. A multiprobe rake, which consisted of a stainless steel, orifice-type gas sample probe, a radiation-shielded, self-aspirated thermocouple probe, and a cone probe for measuring static and total pressure, was installed in the test section.

2.1 COMBUSTOR SYSTEM AND TEST SECTION

The plenum, which encloses the combustor (Fig. 1), was connected to a high-pressure air supply by a 7.62-cm-diam insulated pipe which contains a control valve upstream of a calibrated critical venturi (2.41-cm diameter), enabling the desired mass flow to be controlled and measured. Downstream of the calibrated venturi a propane-fired heat exchanger heated the inlet air to the desired temperature. The heater is capable of heating 2.27 kg/sec of nonvitiated air up to 811°K at a pressure up to 827 kPa. The insulated air supply line was connected to a 40.6-cm-diam plenum section in which an AVCO-Lycoming cylindrical (14-cm diameter) combustor was housed (Fig. 1). The combustor exhausted into the test section through a standard ASME long radius convergent nozzle having an exit diameter of 5.5 cm. A pressure-controlled tank supplied JP-4 fuel to the combustor as shown in Fig. 2, and the flow was measured by two turbine flowmeters.

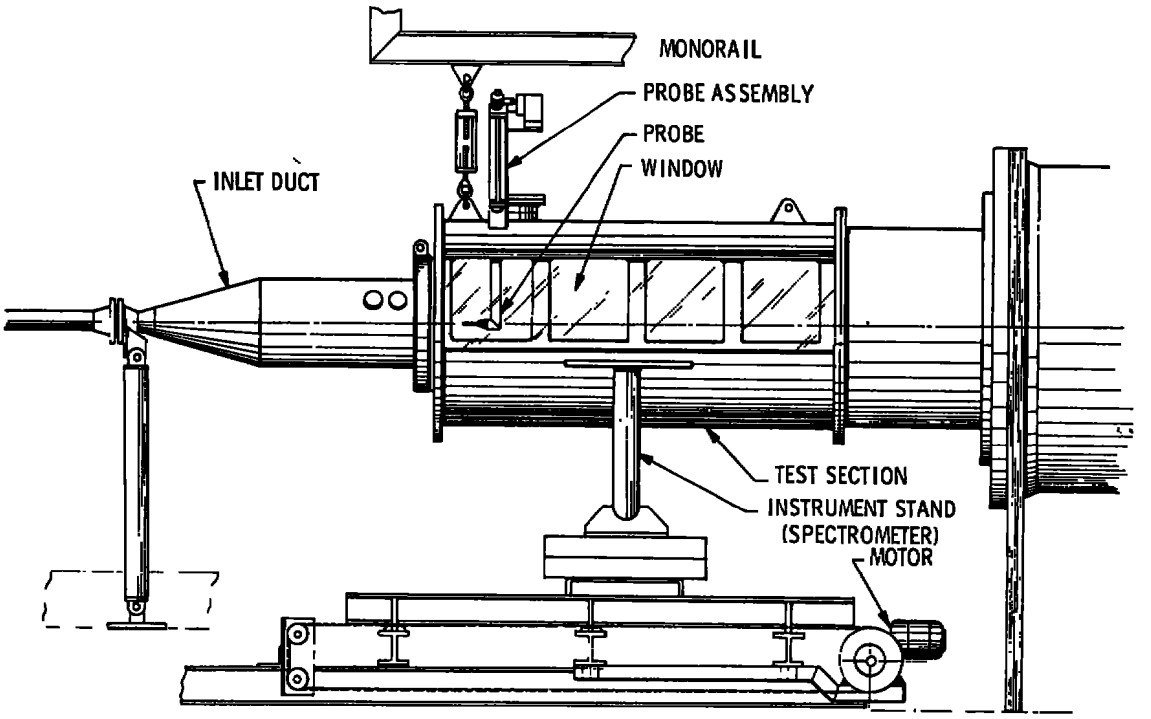

Figure 1. Diagram of R-2C-1 Research Cell.

Test cell and combustor monitoring and operating instrumentation consisted of conventional pressure transducers, gages, and thermocouples. The operation was performed in a control room located adjacent to the test area. The critical operating variables (plenum pressure, air supply temperature, etc.) and monitoring parameters (wall temperatures, etc.) were recorded by an online digital data acquisition system and were displayed in the control room on a cathode ray tube (CRT). Airflow rate, fuel-to-air weight-flow ratio, and combustor temperature were computed on line from measured variables and were displayed on the CRT. Estimates of the uncertainty in measured and calculated combustor operating parameters are given in Table 1. These uncertainties were determined using the method of Ref. 5.

The test section included a controlled secondary airflow system, consisting of an open area of 1,400 cm^2 in the upstream flange portion of the test cell (Fig. 1). The test section was operated at pressures slightly less than atmospheric by means of the ETF exhausters. The exhausters maintain a cell pressure of 92.36 kPa, which results in a secondary airflow of 66 kg/sec. This was sufficient to prevent recirculation of the exhaust gases into the region of the test section where optical measurements were made. The test section contained optical viewing ports (30 x 182 cm) on either side of the test section, as shown in Fig. 1.

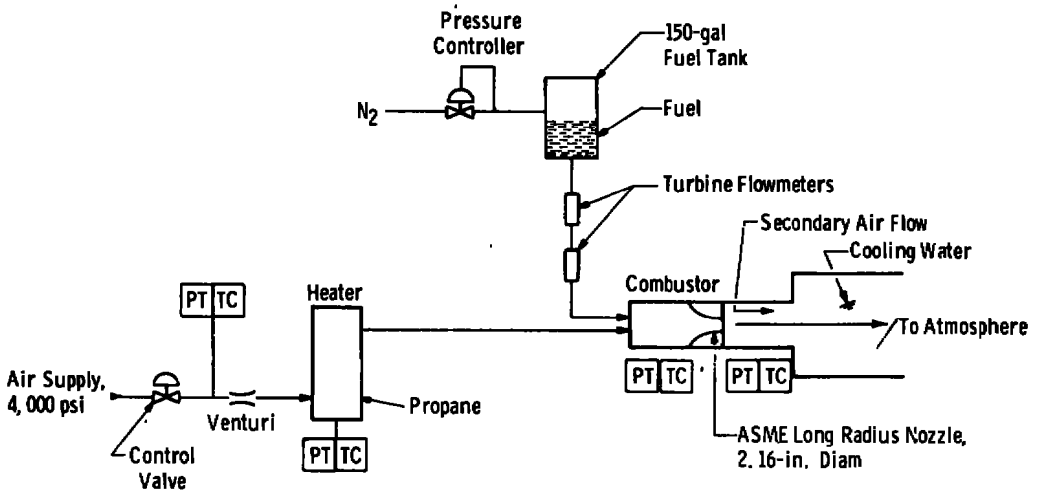

Notes:

1. Weight Flow Measurement
   Calibrated Venturi - 5 lb/sec (max)
2. Propane Heater
   Pressure Limit - 120 psia
   Temperature - 1,000°F (max)
3. PT Pressure Transducer
   TC Thermocouple

Figure 2. Diagram of the R-2C-1 air and fuel supply system.

Table 1. Estimates of Uncertainty for Combustor Operating Parameters

Parameters	Units	Nominal	Precision, percent	Bias, percent	Uncertainty, percent
Air Mass Flow Rate ($\dot{m}_a$)	kg/sec	0.91	±0.14	±0.46	±0.75
Fuel Mass Flow Rate ($\dot{m}_f$)	kg/sec	0.018	±0.75	±2.00	±3.50
Fuel to Air Ratio (f/a)	—	0.02	±0.80	±2.10	±3.70
Combustor Pressure (P_o)	kPa	345	±0.10	±0.30	±0.50
Test Section Pressure (P_c)	kPa	92.00	±0.10	±0.30	±0.50
Inlet Air Temperature	°K	588	±0.10	±0.40	+0.40, +0.6°K

Mounted below the test section, as shown in Fig. 1, was a movable yoke with mounting plates approximately 150 cm apart, which could be positioned at any height, or traversed continuously in the vertical direction across the test section. The yoke could also be positioned at any axial point of the exhaust plume from the combustor nozzle exit to 30 nozzle diameters downstream. The in situ optical measurement devices (consisting of a source and receiver) were mounted on the yoke and were aligned to view a small path (1-cm diameter) through the exhaust plume (Fig. 1). The spectral measurement could be made on plume centerline (any desired axial position), or a horizontal traverse could be made of the plume at fixed wavelength. The multiprobe rake, Fig. 3, was located in the test section so that the probe entrance plane coincided with that of the optical path. The probe could be positioned to coincide with that of the optical measurement at any one of the predetermined instrument locations (Fig. 4) axially across the exhaust plume radius or located at any desired radial position in the exhaust stream.

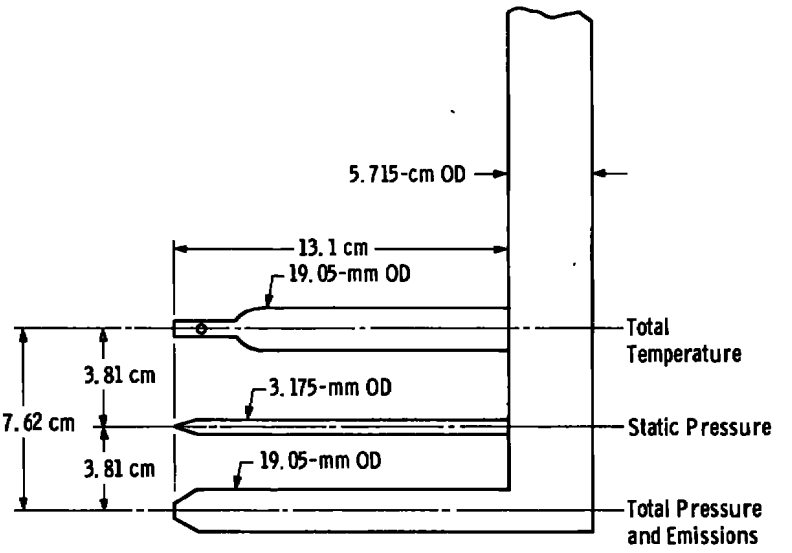

Figure 3. Diagram of the multiprobe rake.

2.2 RESONANCE ABSORPTION SYSTEM

The in situ resonance absorption system, located as shown in Fig. 1, consisted of a resonance lamp source, with transmitting optics located on one side of the test cell and receiving optics and a 0.5-m spectrometer receiver located on the other. The source was a high voltage (3,000-v DC) capillary discharge tube through which a 12:3:1 mixture (by volume) of $A:N_2:O_2$ flowed at a pressure of 0.8 kPa. The discharge tube was water cooled to provide a low-temperature gas mixture, thus ensuring a narrow line source. The spectrometer (receiver) used in this experiment was a 0.5-m Czerny-Turner type mount,

grating instrument with a 2,360 groove/mm grating blazed for maximum reflection at 300 nm. The spectrometer was equipped with curved slits which were opened to 20 nm. The 20-nm slit width resulted in a 0.16-nm bandpass for the instrument. An RCA 1P28 photomultiplier tube was used as a detector.

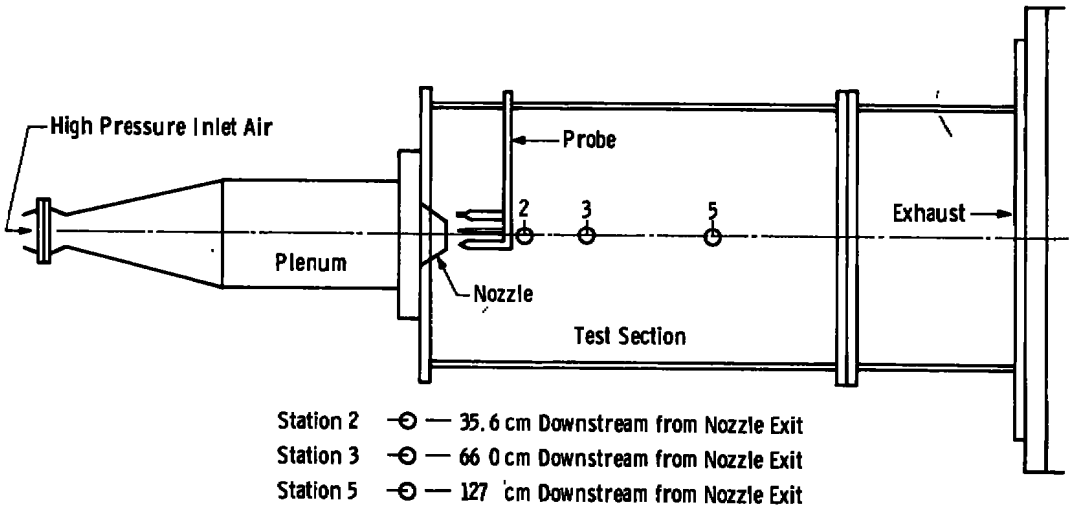

Figure 4. Diagram of R-2C-1 instrumentation stations (probe and spectrometer).

2.3 GAS ANALYSIS SYSTEM

The Society of Automotive Engineers E-31 committee has established guidelines for the design of sample systems and testing approaches to be used in the acquisition of emissions data on turbine engines. These guidelines are contained in Aerospace Recommended Practice (ARP) Number 1256 (Ref. 6) and were adhered to in the design of the AEDC emissions measurement system (Ref. 7). A flow diagram of the analysis system is shown in Fig. 5. The gas sample passes through the heated transfer line, which is maintained at 422 ± 10°K, and into the five analysis instruments. The flow rate through each instrument and the flow rate through the excess line were measured using volume flow, ball-type flowmeters. The analysis panel used in this study contained five types of instruments. The types and models of these instruments were as follows:

1. NO chemiluminescence type, TECO (Model 10A, quoted accuracy ±1 percent)

2. NO_x chemiluminescence type, TECO (Model 10A with converter, quoted accuracy ±1 percent)

3. CO nondispersive infrared type, Beckman (Model 846, quoted accuracy ±1 percent)

4. CO_2 nondispersive infrared type, Beckman (Model 315A, quoted accuracy ±1 percent)

5. C_xH_y flame ionization detector type, Beckman (Model 402, quoted accuracy ±1 percent)

The analyzer instruments were calibrated in-place using certified calibration gases (supplied by the Scott Research Corpration). A gas to establish an instrument zero and a minimum of two different calibration gases were used in the calibrations. The accuracy of the concentration of the calibration gas was estimated to be ±2 percent (Ref. 8). Temperature conditioning was provided within the analyzer by steam-jacketed lines designed according to the ARP-1256 standards (Ref. 6). Standard pressure and temperature instrumentation were used to insure operation of both the analyzer and the entire emission measurement system in accordance with manufacturer's instructions. The overall estimated uncertainty of the emission data presented is ±10 percent of the values shown.

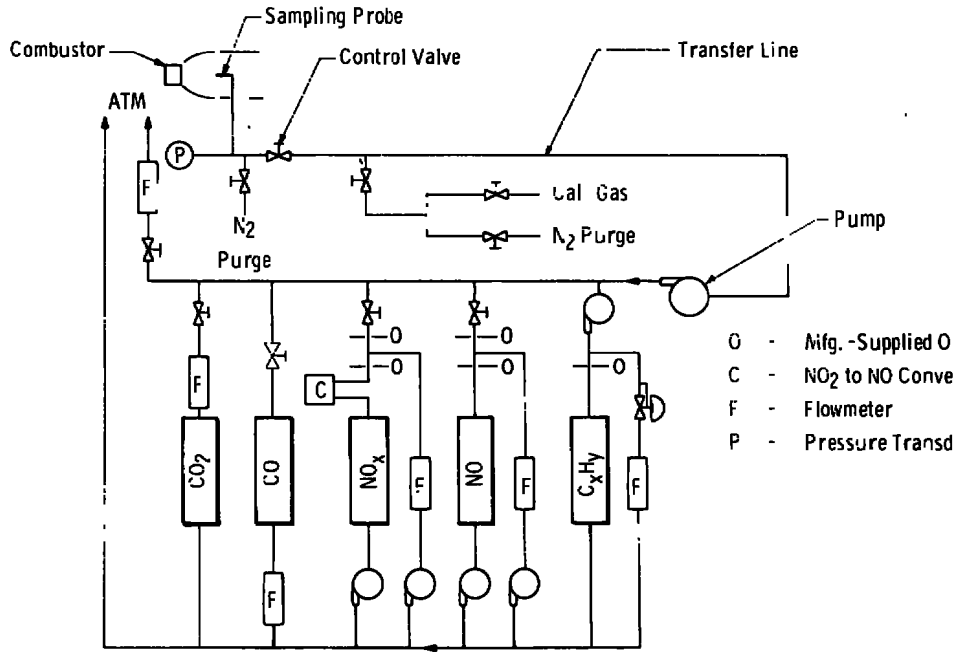

Figure 5. Diagram of gas analysis system.

2.4 MULTIPROBE RAKE

The determination of the exhaust stream gas properties, static pressure (p) and temperature (T_a), is required in the reduction of the optical measurements. The multiprobe rake was designed to provide the data for the calculation of these properties

as well as the emissions data. The rake consists of three different probes mounted on a traversing mechanism which was described in Section 2.0.

The emissions probe used in these studies was an orifice type of 0.95-cm-ID stainless steel tubing enclosed within a liquid-cooled housing (Fig. 6a). A metal bellows pump was located in the sample gas transfer line and maintained a low pressure in the emission probe of approximately 41.4 kPa for all measurement stations. The coolant was supplied by a high-pressure pump (1,240 kPa) from a reservoir containing a mixture of water and ethylene glycol. The temperature of the mixture was controlled by a series of electrical heaters located within the reservoir.

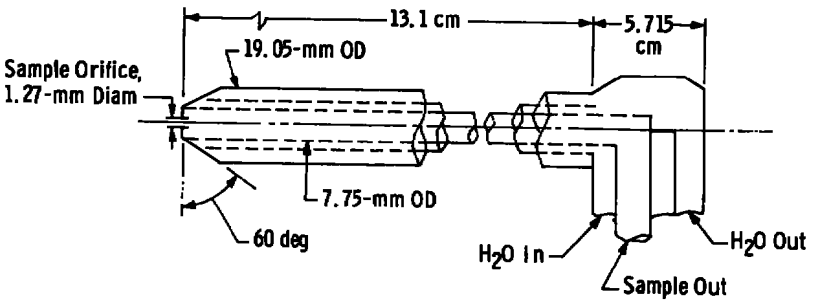

a. Emissions probe and total pressure probe

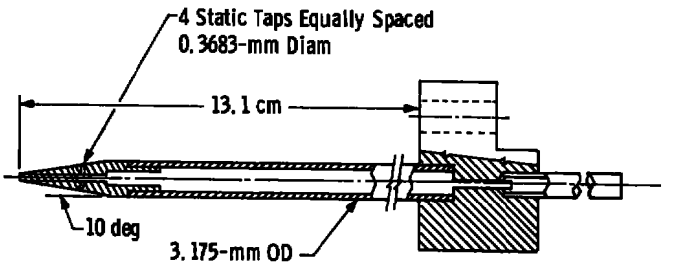

b. Static pressure probe

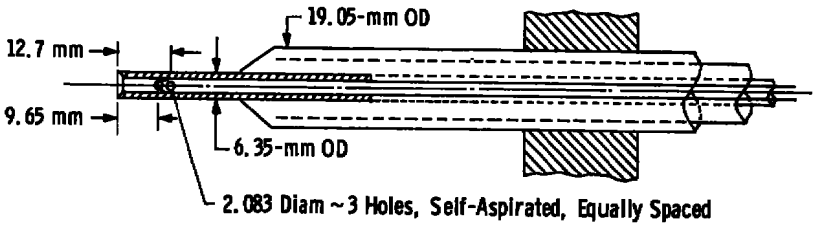

c. Total temperature probe

Figure 6. Diagram of static pressure, total temperature, and emissions probes.

The emissions probe (Fig. 6a) served as the total pressure probe by closing an isolation valve in the gas sample transfer line. A pressure transducer was located upstream of this isolation valve, and total pressure was recorded by an online digital data acquisition system and displayed on a CRT in the control room.

A cone probe (Fig. 6b) was designed and employed to measure static pressure, p, in the combustor exhaust stream. This pressure was also recorded on the online digital system and displayed on the CRT.

The total temperature probe (Fig. 6c) was a self-aspirated, radiation-shielded, Chromel®-Alumel® (C/A) thermocouple probe. A recovery factor of 0.81 was used in determining gas temperature from the measured thermocouple junction temperature. The signal was recorded as mentioned above and displayed on the CRT.

The multiprobe rake containing the previously described probes (total pressure, static pressure, and total temperature) provided the measurements of the required parameters for the calculation of the static temperature profiles using the isentropic flow equation. The Mach number (M) used in this calculation was obtained from measured total and cone probe pressures by interpolation from the cone probe calibration curve (Fig. 7).

2.5 LOW-PRESSURE PROBE SYSTEM FOR NO

The operation of the chemiluminescence type of NO concentration analyzer depends on monitoring the output of light from the chemiluminescent reaction in a low pressure (~1.3 kPa) chamber between the NO in a gas sample and O_3 generated within the instrument. Ordinarily, the gas sample is not reduced in pressure until just before it enters the reaction chamber; however, the work of Stedman (Ref. 3) has indicated that the accuracy of the NO concentration measurements made with a probe in laboratory experiments could be improved by maintaining the gas sample at a low pressure (~1.3 kPa) from the time it enters the probe until it exits the reaction chamber. To see whether lowering the pressure of the gas sample at the probe entrance would furnish different results for the NO concentration measurements, a low-pressure gas-sampling probe system (Fig. 8) was fabricated using a Thermo Electron Corp. Model 10A chemiluminescent NO analyzer. In addition to the NO analyzer, this system is comprised of (1) an uncooled quartz sampling probe with a 0.033-cm-diam inlet orifice, (2) a stainless steel sample transfer line, (3) a flowmeter for determining sample and calibration gas flows into the system, (4) a calibration gas system, (5) a vacuum pump for the reaction chamber, and (6) a vacuum pump to bypass part of the gas sample.

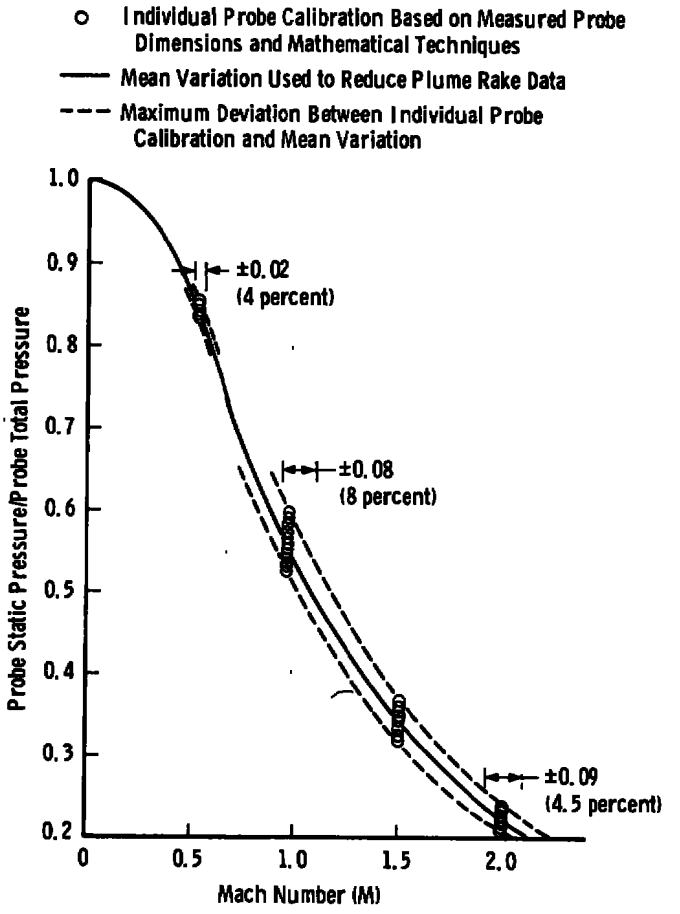

Figure 7. Exhaust plume rake cone probe calibration curve.

The operation of the low-pressure sampling system required that both vacuum pumps be running and that the valve to the bypass vacuum pump be adjusted until a reading of about 1.3 kPa was obtained on the sample line pressure gage. This action established a flow of sample through the system, and the vacuum pump connected to the reaction chamber of the analyzer pulled a portion of the sample into and through the reaction chamber. The sample regulator functioned to help hold a constant pressure in the reaction chamber so that fluctuations in the flow through the chamber were minimized. When a constant flow rate was established through the system, the amount of flow through the flowmeter was recorded. The sample line was then closed by the shutoff valve, and the calibration gas valve was opened. The calibration gas flow was set at the same value that was set to read the calibration gas value. A zero level for the analyzer was set by shutting off the calibration gas and introducing dry nitrogen gas into the analyzer. The calibration system was then shut off and the sample system reopened, and after it was determined that the same flow and pressure existed in the sampling system, the NO concentration level was recorded.

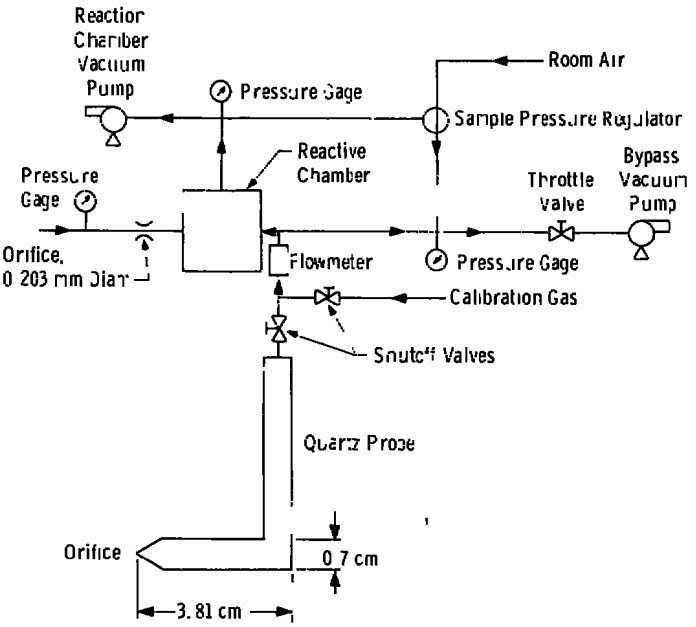

Figure 8. Diagram of low-pressure gas analysis probe.

2.6 PROBE SIMULATOR EXPERIMENT

Work done by Benson and Samuelsen (Ref. 4) indicates that the concentration levels of NO and CO in a gas sample could be influenced by the temperature of the surface in contact with the sample in the presence of H_2. The results of this work indicate the existence of one possible mechanism by which NO could be destroyed in a gas sample and have prompted the fabrication of an apparatus which simulates the entrance region of a probe immersed in a hot gas stream with which an experiment similar to that of Ref. 4 was performed. This apparatus is shown in Fig. 9. It consisted of (1) a stainless steel tube with lugs welded to the tip of the tube which were connected to a welding machine to resistance heat the tube tip to different temperatures, (2) a C/A thermocouple attached to the outside surface of the stainless steel tube between the heating lugs which monitored the tube temperature, and (3) a stainless steel plenum around the tube entrance which was supplied with inlet fittings through which different calibration standard gases were introduced as the gas source. The stainless steel tube was connected to the gas analysis instrumentation described in Section 2.3.

The probe simulator experiments were initiated by introducing calibration gases with different constituents contained in N_2 carrier gas, each of which was known to exist in the exhaust stream, in known ratios to give gas samples of known emissions concentrations at ambient temperatures. These ratios were set by monitoring the different constituents on the gas analysis instrumentation and adjusting calibration gas flows until

the desired proportions of the known concentrations were achieved. The flows also went through tapered tube and float-type flowmeters so that flows could be maintained constant. Once the proper gas flows were established, the temperature of the sampling tube inlet was varied by varying the current flow from the welding machine through the tube tip. A probe tip temperature versus gas sample emissions concentrations history was then obtained for several different gas mixes.

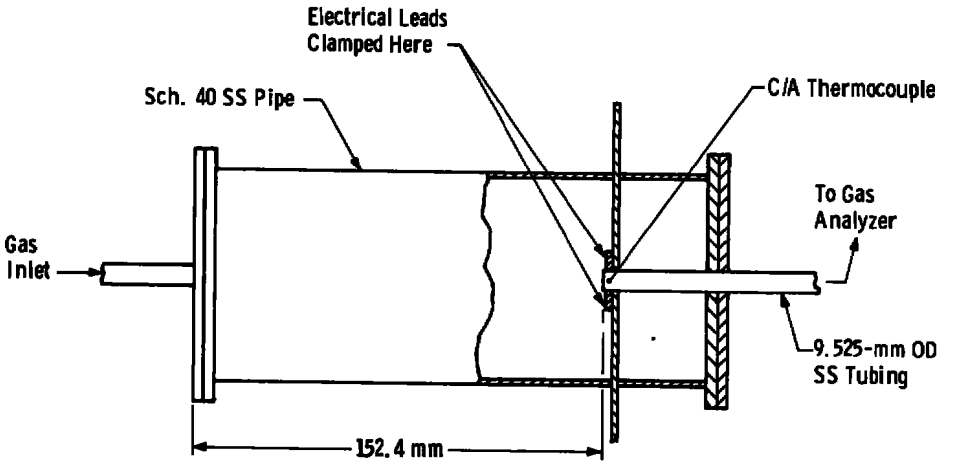

Figure 9. Diagram of probe simulator.

3.0 DESCRIPTION OF ULTRAVIOLET RESONANCE LINE ABSORPTION METHOD: THEORETICAL CONSIDERATIONS

The resonance line absorption technique for the measurement of species concentrations has been treated elsewhere (Refs. 9, 10, and 11). It involves the relationship between the transmittance at some wavelength and the properties (species number density, temperature, and pressure) of the gas in the absorbing path. The transmissivity, t [in a given frequency interval ($\Delta\nu$) of a gas of pathlength (ℓ) containing a density (N) of NO molecules] of radiation from a source which emits only radiation from the γ bands of NO is given by

$$t_{\Delta\nu} = \frac{\sum_j I^\circ_{\nu_j^\circ} \int_o^\infty \exp\left\{-\left[\frac{2\sqrt{\ell n\, 2}\ (\nu - \nu_j^\circ)}{(\Delta_s \nu_j)_D}\right]^2\right\} \exp\left\{-\frac{\ell}{\pi}\sum_i k_{\nu_i^\circ} \int_{-\infty}^{\infty} \frac{a' e^{-y^2}\, d\nu}{a'^2 + (\omega_i - y)^2}\right\} d\nu}{\sum_j I^\circ_{\nu_j^\circ} \int_o^\infty \exp\left\{-\left[\frac{2\sqrt{\ell n\, 2}\ (\nu - \nu_j^\circ)}{(\Delta_s \nu_j)_D}\right]^2\right\} d\nu} \quad (1)$$

For the (0,0) γ bands of NO, the Doppler absorption coefficient at line center is related to the number density of absorbers as follows:

$$k^{\circ}_{\nu_i^{\circ}} = 1.603 \times 10^{-14} \frac{S_i N}{T_a^{3/2}} \exp\left[-1.438 \frac{F_i}{T_a}\right] \tag{2}$$

The derivation of Eqs. (1) and (2) is given in detail in Ref. 12.

In Eqs. (1) and (2) are one measurable quantity, t, and three unknown properties of the gas, N, T_a, and p. The remainder of the terms are physical constants or known molecular properties. The pressure enters the derivation only as it affects the line-broadening parameter a'. If the pressure and temperature are known, then N can be obtained from the measurement. Note that the equation holds only for a homogeneous gas; however, if the path length through the gas is nonhomogeneous but has known profiles of N, T_a, and p, then the transmissivity can be calculated by summing along the path, assuming increments, $\Delta\ell$, of uniform properties.

The inverse problem, determination of N along the optical path from measurements of t, T_a, and p along a path having nonuniform properties, can be solved in some cases. One such case is that of cylindrical symmetry in which concentric zones of constant properties can be assumed and a measurement of transmission is made through chords along the vertical directions, as illustrated in Fig. 10. For the case of cylindrical symmetry, an inversion procedure can be applied when the transmissivity profile t(x) has been measured and T(r) and p(r) are known (Fig. 10). In the experiment reported here, cylindrical symmetry was maintained at all measurement stations. An iterative computer program was used (Ref. 11) which proceeded as follows:

1. The cylindrical gas stream was divided into m concentric zones, and a known temperature, T_m, and pressure, p_m, were consigned to each zone, m (see Fig. 10).

2. The average path length of each zone was calculated from geometrical considerations and knowledge of the optical beam size.

3. The number density of the outer zone was calculated from the measured transmissivity, t_1, and known T_1 and p_1, using Eq. (1).

4. Using the "known" outer zone NO number density, N_1, and measured T_2 and p_2, the second zone number density, N_2, was determined by guessing a value of N_2, computing t_2, the second zone transmissivity, re-guessing N_2, and proceeding until the computed and measured t_2 values converged to within 0.0001.

5. The procedure in step 4 was repeated to obtain N_2', N_3,...until the entire radial profile was obtained. The estimated uncertainty of the optical results presented is ±10 percent of the values shown.

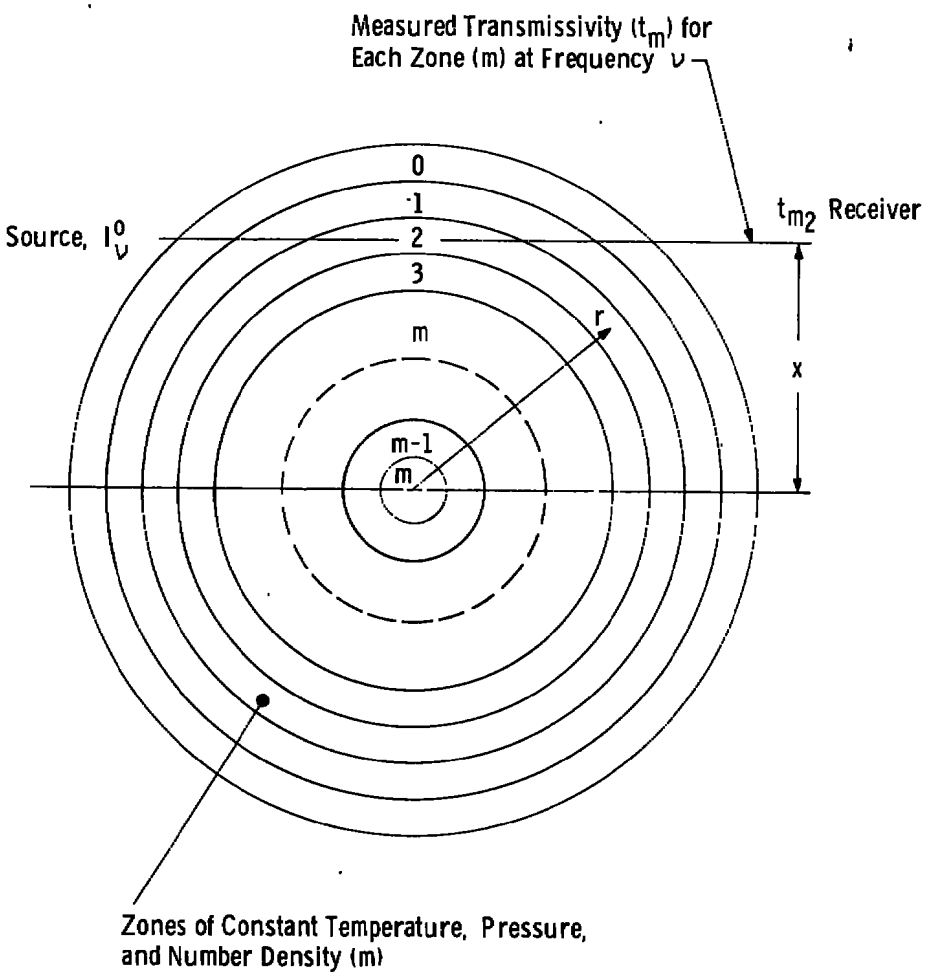

Figure 10. Illustration of radial inversion problem for determination of local concentration from transmissivity measurements.

4.0 RESULTS AND DISCUSSION

The multiprobe rake radial profile measurements of emissions, total pressure, total temperature, and static pressure, and the NO optical measurements were made at test stations located 35.6, 66, and 127 cm downstream from the nozzle exit plane.

The combustor operating conditions are presented in Table 2 as a function of measurement station. The inlet air temperature, which was 14 percent lower for the

Table 2. Emissions Concentrations Measured with Orifice Probe

Sta.	r/R_n	Fuel to Air Ratio	Airflow, kgm/sec	Inlet Air Temp, °K	Combustor Pressure, kPa	NO Content, ppmv	NO_x Content, ppmv	CO Content, ppmv	CO_2 Content, percent	C_xH_y Content, ppmc
5	℄	0.020	0.909	589	345.7	15	16.1	10.9	0.67	12.4
↓	1.85	↓	↓	↓	↓	12	11.6	5.5	0.49	12.2
↓	3.70	↓	↓	↓	↓	7	7.5	0	0.30	10.3
↓	5.56	↓	↓	↓	↓	4	4.1	0	0.14	10.4
↓	7.41	↓	0.908	↓	↓	3	1.8	0	0.06	10.4
↓	9.26	↓	0.907	↓	345.3	2	4.2	0	0.03	8.8
↓	11.10	↓	0.907	↓	350.8	0	1.3	0	0.03	9.0
3	℄	↓	0.910	↓	347.4	34	35.6	64.8	1.35	7.3
↓	1.85	↓	0.908	↓	346.7	20	21.7	28.5	0.92	7.3
↓	3.70	↓	0.909	↓	↓	5	5.2	4.1	0.26	7.4
↓	5.56	↓	0.910	↓	↓	0	0.7	0	0.07	7.7
2	℄	↓	0.908	505	337.1	55	63.3	302	3.14	6.9
2	1.85	↓	0.909	505	337.8	14	21.2	116	0.89	8.9

[a]Note: Test Cell Pressure = 92 kPa

station 2 measurements than for the stations 3 and 5 measurements, may influence the NO production in the combustion process and make comparisons as a function of station location difficult. However, the purpose of these tests was to compare the optical and probe results for a given set of combustor conditions. Although the inlet temperature at station 2 was lower than that at the other stations, the probe and optical measurements were made at the same combustor conditions at stations 3 and 5.

4.1 PROBE MEASUREMENTS

The gas sampling system contained standard instrumentation to measure concentrations of NO, NO_x, CO, CO_2, and C_xH_y. The results of emissions concentrations measured with the orifice probe are presented in Table 2. For the purpose of this study, only NO and CO_2 data are of concern.

The quality of the probe emissions measurements was placed in question when a leak was discovered in the sample gas transfer line pump after completion of the test. A posttest correction was made by determining the amount of dilution experienced at different inlet pressures on the orifice probe. This was accomplished by simulation of the inlet pressure to the probe with a known NO calibration gas. The correction was applied to the measured species concentrations obtained from the exhaust stream. The uncertainty of ±10 percent placed on the results reflects this consideration.

The static pressure probe failed during the test, and the assumption of a constant static pressure measurement equal to the cell (ambient) pressure had to be made for all stations. The static pressure is used in the broadening parameter (á) and in the calculation of the local jet exhaust Mach number.

The Mach number at each location was determined by using the assumed constant static pressure (equal to ambient test cell pressure) and calculating the Mach number as a function of the assumed static-to-measured total pressure ratio with a variable value for γ. The static temperature was calculated using the measured total temperature and the Mach number previously calculated.

Radial distributions of static temperature, static pressure, and percent transmission are shown plotted versus r/R_n (where R_n is the nozzle radius and r is the radial distance from exhaust stream centerline) in Figs. 11, 12, and 13 for various downstream stations. Radial distributions of NO concentrations obtained by the sample probe and optical technique are shown for comparison in Figs. 14, 15, and 16.

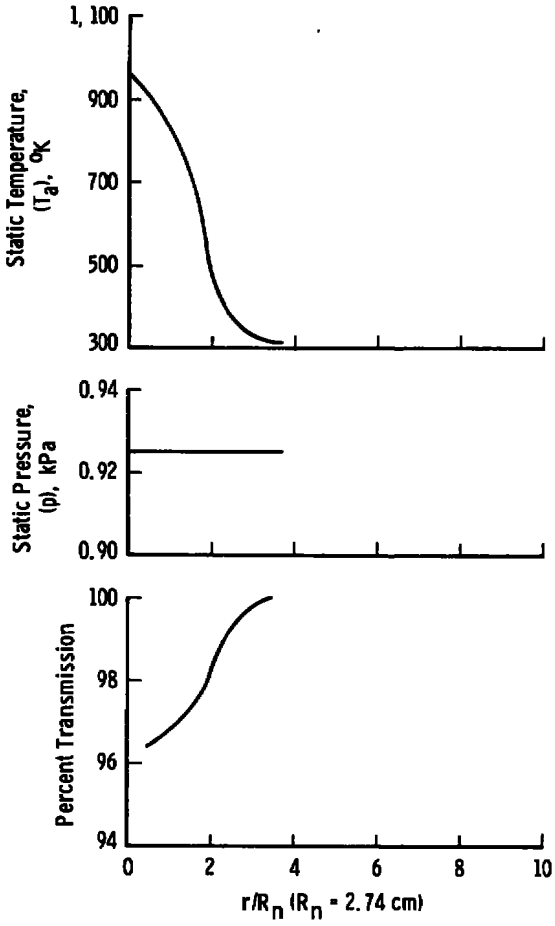

Figure 11. Static temperature, static pressure, and percent transmission plotted as a function of radius for an example combustor condition at station 2.

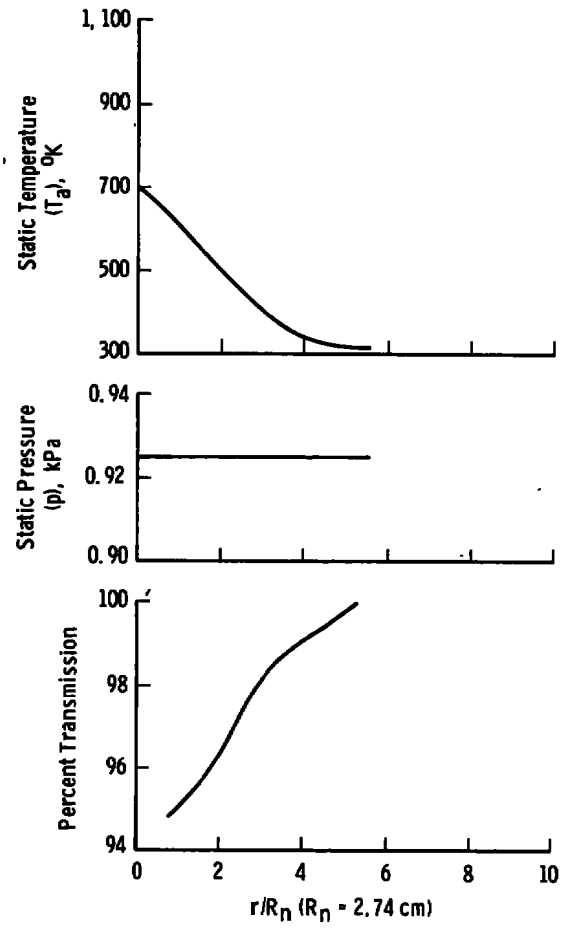

Figure 12. Station temperature, static pressure, and percent transmission plotted as a function of radius for an example combustor condition at station 3.

A momentum balance was performed to evaluate the consistency of the pitot pressure measurements and the assumption of constant radial static pressure. The calculation was made for a cylindrical duct (test section) assuming no wall friction according to

$$\int_0^{r_{wall}} \rho_u (u - u_o)\, r\,dr + \int_0^{r_{wall}} (p - P_o)\, r\,dr = \left[\rho_j u_j (u_j - u_o) + (p_j - P_o)\right] \frac{A_j}{2\pi} \quad (3)$$

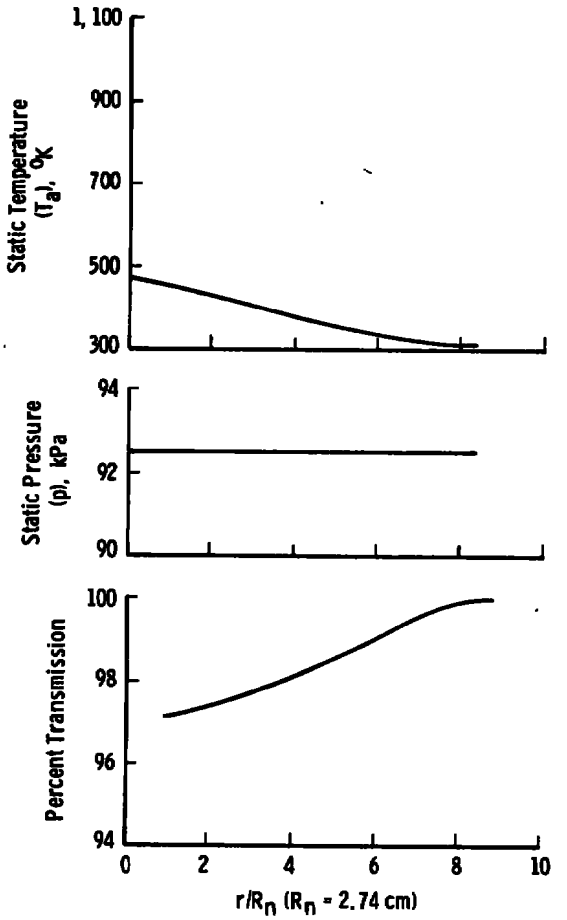

Figure 13. Static temperature, static pressure, and percent transmission plotted as a function of radius for an example combustor condition at station 5.

The right-hand side of this equation depends only on the jet properties and the external velocity and pressure and is a constant for a given set of test conditions, and therefore the sum of the two integrals on the left-hand side is a conserved quantity with measuring station. With the additional assumption of constant static pressure, the pressure difference in the second integral goes to zero and $\int \rho u\ (u - u_o)\ rdr$ becomes a constant independent of the axial distance.

The results of this calculation are shown in Fig. 17. As can be seen, the integrated momentum does remain essentially constant for stations 2 and 5. However, there is a significant increase in momentum shown for station 3 that could be a result of a measuring error in total pressure, total temperature, determination of the jet boundary, or the assumption of constant static pressure.

The low-pressure probe was used to measure the NO concentration at the centerline of the combustor exhaust at an axial position 66 cm downstream of the nozzle exit plane (station 3). An NO concentration level of 36 ppmv was obtained at this position, and this value compares with a level of 34 ppmv obtained at the same position with the orifice probe. These results indicate that for these conditions, no differences in NO concentration measurements were observed between the low-pressure probe and the orifice probe. These results are within the measuring uncertainties even though two separate systems were employed.

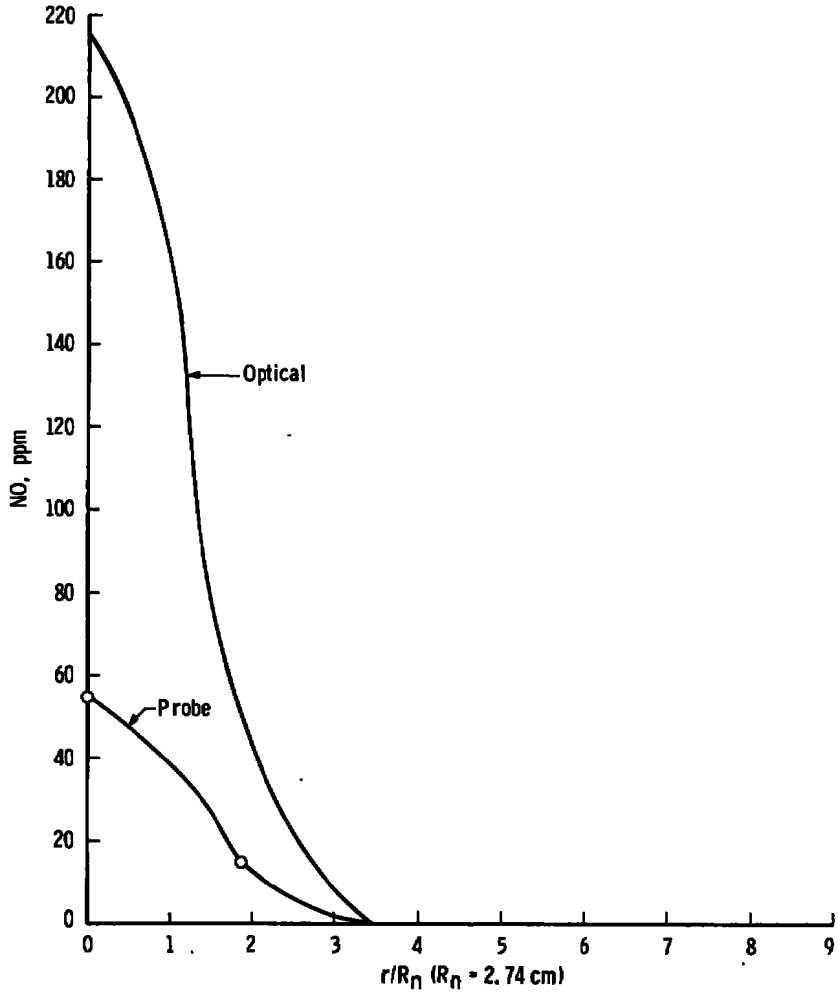

Figure 14. Optical and probe NO concentrations plotted as a function of radius at station 2.

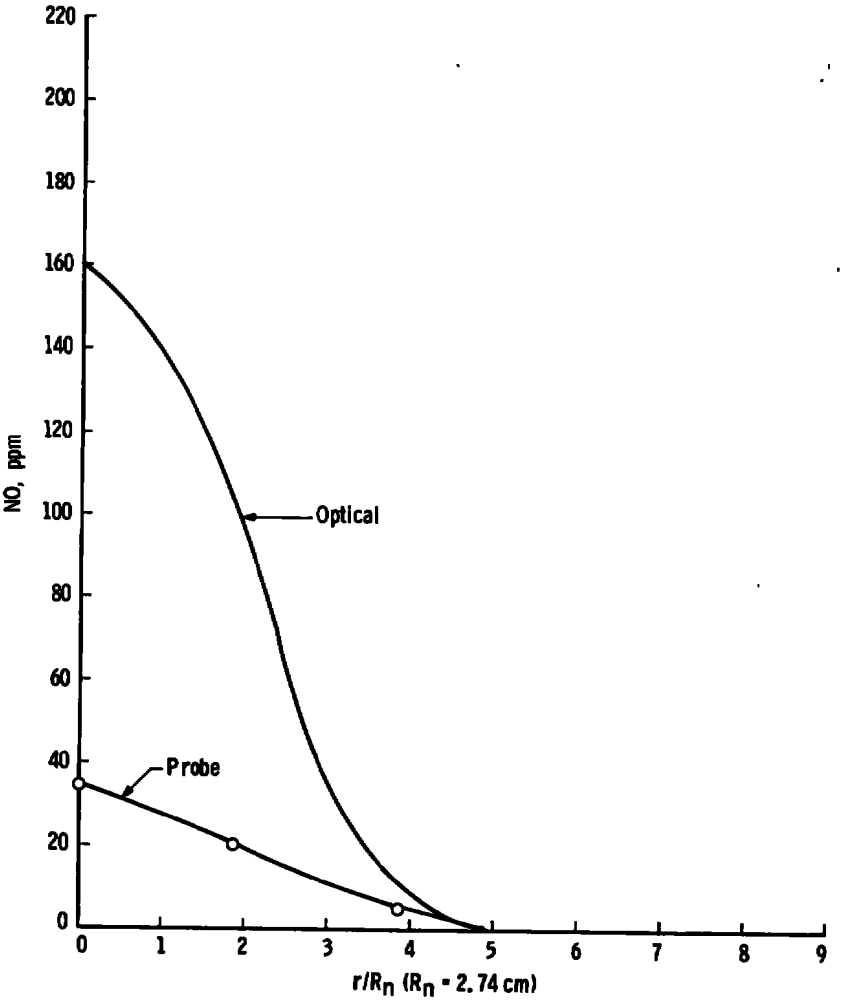

Figure 15. Optical and probe NO concentrations plotted as a function of radius at station 3.

4.2 OPTICAL MEASUREMENTS OF NO CONCENTRATIONS

The UV optical system was used to obtain optical transmissivity data from the measurement stations described previously. Spectral scans of the (2,2) bandhead of NO were also obtained in order to correct for extraneous absorption (including particulate scattering, source drift, etc.) in the combustor exhaust system.

The data reduction was accomplished as outlined in Section 3.0. The results of the data reduction procedure yield the (corrected) transmissivity of the (0,0) γ-band for that line of sight. The measurements are repeated through several chords of the exhaust stream, and the data are then inverted as discussed previously to obtain the radial profile

of NO concentration. The percent transmission data for various measurement stations are shown in Figs. 11, 12, and 13. The results of inverting the transmission data at various stations to local values of NO concentration are given in Figs. 14, 15, and 16 for comparison with probe measurement values. It is shown in these figures that the centerline ratio of the optical- to probe-measured NO concentration varies as the measurements progress downstream. The ratios varied from approximately four at the 6.5 nozzle diameter station (station 2) to about two at the 25 nozzle diameter station (station 5). The centerline static temperature at these stations was calculated and found to decrease from 950 to 470°K, respectively.

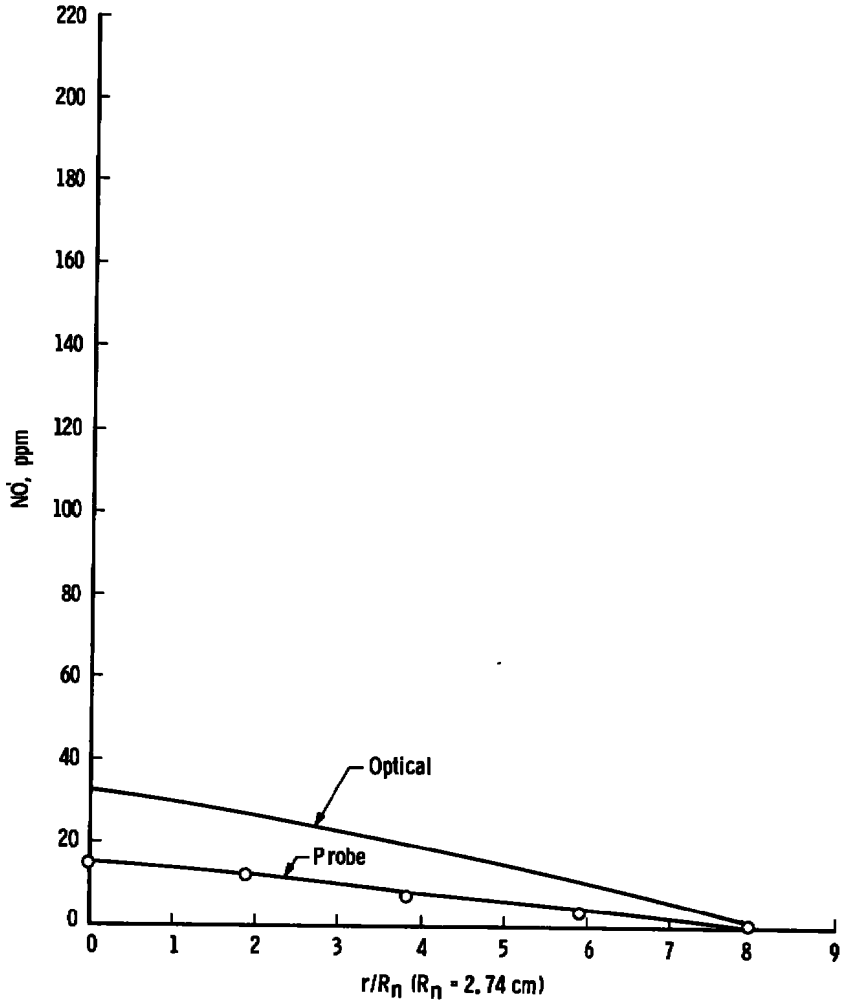

Figure 16. Optical and probe NO concentrations plotted as a function of radius at station 5.

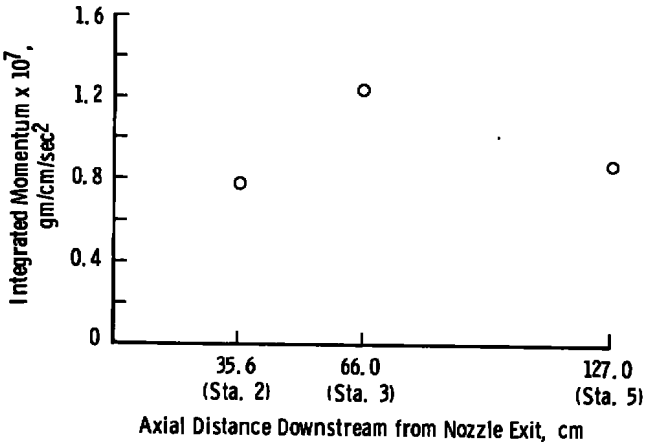

Figure 17. Integrated momentum versus axial distance downstream from nozzle exit.

4.3 COMPARISON OF PROBE AND OPTICAL RESULTS

The NO concentrations determined by the probe and optical techniques are plotted in Fig. 18. The optical data were selected for presentation at the location in the exhaust jet where the probe data were taken. Therefore, the data presented are at the same radial and axial location in the jet exhaust. For the data presented in Fig. 18, the optical results are from 2 to 4 times larger than the probe results, depending on the optical measuring station.

A further analysis was performed to investigate the possibility of gas phase NO reactions occurring in the exhaust stream. The amount of any specie in the exhaust stream which passes through a cross-sectional area of the exhaust per unit time can be expressed from the continuity equation as

$$\dot{m}_s = 2\pi \int_0^N C_s \sqrt{\frac{\gamma}{RT_a}}\, p_j\, M\, r\, dr \qquad (4)$$

Equation (4) may be evaluated for the specie of interest, C, at each measurement station since calculated values of p, T_a, and M are available. [Evaluation of Eq. (4) can be accomplished by plotting the function inside the integral sign and determining the area thus formed by using a planimeter.]

The results obtained for the NO flux at each measurement station in the exhaust from the measured concentrations furnished by the probe and by the in situ technique are shown in Fig. 19. Also included in Fig. 19 is a calculation of the CO_2 flux

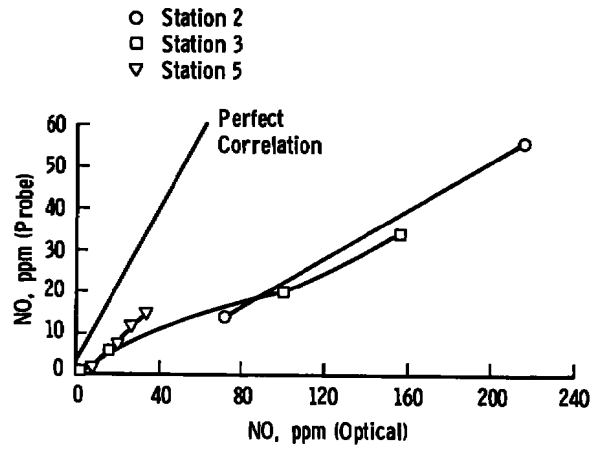

Figure 18. Concentration of NO measured by probe versus concentration of NO measured optically.

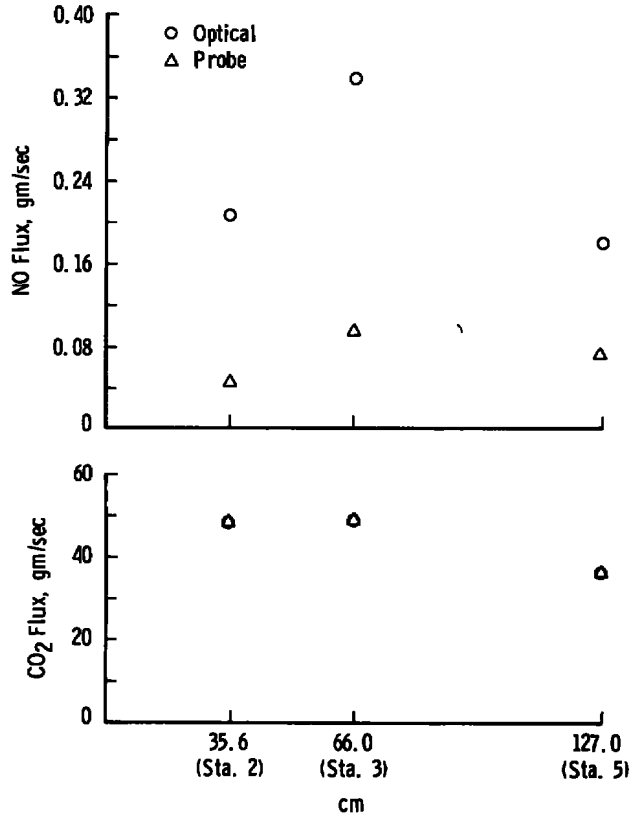

Figure 19. Total flux of CO_2 and NO determined by sample probe and optical techniques versus axial distance downstream from nozzle exit.

determined from the probe-measured concentrations at each measurement station in the exhaust stream. The probe CO_2 flux calculation is included to help check the validity of the probe-determined values of NO because the CO_2 should be inactive in the exhaust stream.

The NO flux values at stations 2 and 5 are about the same for each of the measuring techniques; however, the optical values are a factor of 3 to 5 times larger than the probe results. The significant increase in the NO flux shown at station 3 for both measuring techniques cannot be explained, but it is consistent with the observed increase in momentum flux shown in Fig. 17. The CO_2 flux values show no significant anomalies with downstream measurement stations.

4.4 PROBE SIMULATOR RESULTS

The changes caused in the emissions concentration level of the input gas samples by the different sampling tube temperatures are shown in Table 3. The results shown in

Table 3. Emissions Concentrations as Functions of Probe Simulator Sampling Tube Temperature and Input Gas Constituents

Run No.	Temp, °K	NO, ppmv	CO, ppmv	CO_2, percent	C_xH_y, ppmc	H_2, percent	O_2, percent
1	Input	518	6	0	95	3.27	0
	311					Not Measured	Not Measured
	422						
	478						
	533				96		
	589	515					
	644	449					
	700	360			95		
	828	308			94		
	617	335			95		
	533	428			95		
	478	493			96		
	422	510			96		
	311	510					
2	Input	402	10	2.51	98	2.96	2.4
	311					Not Measured	Not Measured
	422				99		
	478				100		
	533	401					
	617	400			99		
	700	400	11		94		
	811	396	22		97		
	867	385	15		98		
	700	395	10		99		
	589	401					
	533	402					
	478						
	422						
	367						
	311						

Table 3 indicate that NO is partially destroyed as sampling tube temperature increases above about 617°K when H_2 is present and O_2 is not present. The presence of O_2 inhibits the NO destruction mechanism for the tube temperature and gas mixes employed in this study. Measured CO concentrations are increased at sampling tube temperatures above about 617°K when H_2 and CO_2 are present; however, in the case of the highest concentration of O_2 used (Run 5, O_2 = 4.2 percent) the measured concentration level was decreased below the input level. While the concentration levels and the constituent gases used in this study may not be totally representative of all conditions to be found in different exhaust plumes, the results presented in Table 3 do indicate that emissions levels in gas samples can be altered by temperature changes of the probe wall.

Table 3. Continued

Run No.	Temp, °K	NO, ppmv	CO, ppmv	CO_2, percent	C_xH_y, ppmc	H_2, percent	H_2, percent
3	Input	245	693	4.52	44	1.52	0
	311	245	693			Not Measured	Not Measured
	422	240	726				
	533	240	730				
	700	206	736				
	756	180	810				
	811	165	908				
	839	160	971				
	700	162	870				
	644	172	799				
	589	185	760				
	533	211	742				
	478	230	734				
	422	242	726				
	311	242	726				
4	Input	208	624	3.87	30	1.03	4.20
	311	208	624			Not Measured	Not Measured
	422	206	630				
	478	210	615				
	533		602	3.88			
	644		573	3.93			
	700		521	3.90	31		
	756		499		31		
	811	208	502		30		
	700	207	516	3.91			
	589	208	544	3.93			
	478	210	597	3.90			
	422		599				
	311		599				

Table 3. Concluded

Run No.	Temp, °K	NO, ppmv	CO, ppmv	CO_2, percent	C_xH_y, ppmc	H_2, percent	O_2, percent
5	Input	206	627	3.80	67	2.31	0
	311	↓	627	↓	↓	Not	Not
	422		624			Measured	Measured
	478	208	625			↓	↓
	533	206	623				
	644	195	633				
	700	175	660				
	756	150	772				
	783	140	872				
	811	132	943				
	644	138	740				
	589	153	641				
	533	175	624				
	478	195	618				
	422	206	↓				
	311	206					
6	Input	406	11	3.90	61	2.10	0
	311	↓	↓	↓	↓	Not	Not
	422					Measured	Measured
	478					↓	↓
	533	400	13				
	644	373	23				
	700	340	58				
	756	301	138				
	828	262	281	3.81	68		
	756	265	185	↓	↓		
	644	290	80				
	589	325	42				
	533	370	22				
	478	400	14				
	422	410	12				
	311	410	12				

5.0 SUMMARY

Measurements of NO concentration by an optical in situ technique and sample probe measurements of NO and CO_2 concentration in the exhaust of a turbine engine combustor were made at various axial positions downstream of the combustor nozzle exit. Also, measurements of the NO concentration in the exhaust were made with a low-pressure probe system and compared to values obtained with the conventional probe system. The combustor was operated at a fuel-to-air ratio of 0.02, inlet air temperatures of 505 and 589°K, and a total pressure of 345 kPa. A study was conducted to determine the effect of sampling tube temperature on the NO and CO contents in a gas sample representative of a combustor exhaust gas sample. The results of these measurements show the following:

1. NO concentrations measured by probe and optical techniques continue to show a difference. The centerline ratio of optical- to probe-measured NO

concentration varied from approximately four at the 6.5 nozzle diameter station to about two at the 25 nozzle diameter station. The present results do not indicate any static temperature regions within the exhaust plume (from ≈ 300 to 950°K) wherein the probe and optical techniques agree.

Integrating the local NO concentration to obtain values of the flux at several downstream stations also shows the optical measurements to be three to five times larger than the probe results.

2. Low-pressure probe measurements of NO concentration did not differ from values obtained with an orifice-type probe.

3. Probe simulator experiments showed that in the presence of H_2, measured concentrations of NO decreased and CO increased as the probe tip temperature was increased.

REFERENCES

1. Few, J. D., Bryson, R. J., and McGregor, W. K. "Evaluation of Probe Sampling versus Optical In Situ Measurements of Nitric Oxide Concentrations in a Jet Engine Combustor Exhaust." AEDC-TR-76-180 (ADA034726), January 1977.

2. Few, J. D. "Optical Measurements of NO and NO_2 in the Exhaust of an F101-GE-100 Engine at Simulated Altitudes." AEDC-TR-77-75 (ADA047882), December 1977.

3. Steffenson, D. M. and Stedman, D. H. "Optimization of the Operating Parameters of Chemiluminescent Nitric Oxide Detectors." Analytical Chemistry, Vol. 46, No. 12, October 1974, pp. 1704-1709.

4. Benson, R. and Samuelson, G. S. "Oxides of Nitrogen Transformation While Sampling Combustor Products Containing Carbon Monoxide and Hydrogen." Presented at the 1976 Fall Meeting, Western States Section, Combustion Institute, University of California, San Diego, October 18-20, 1976.

5. Thompson, J. W., Jr. and Abernathy, R. B., et al. "Handbook: Uncertainty in Gas Turbine Measurements." AEDC-TR-73-5 (AD755356), February 1973.

6. SAE Aerospace Recommended Practice 1256, "Procedure for the Continuous Sampling and Measurement of Gaseous Emissions from Aircraft Turbine Engines." Society of Automotive Engineers, New York, October 1, 1971.

7. Davidson, D. L. and Domal, A. F. "Emission Measurements of a J93 Turbojet Engine." AEDC-TR-73-132 (AD766648), September 1973.

8. Williamson, R. C. and Stanforth, C. M. "The Evaluation of Factors Which Influence Accuracy Based Upon Experience in Measurements of Aircraft Exhaust Emissions". Presented at the Third Joint Environmental Instrumentation and Control Symposium, New York, October 1974.

9. McGregor, W. K., Few, J. D., and Litton, C. D. "Resonance Line Absorption Method for Determination of Nitric Oxide Concentration." AEDC-TR-73-182 (AD771642), December 1973.

10. Davis, M. G., McGregor, W. K., and Few, J. D. "Spectral Simulation of Resonance Band Transmission Profiles for Species Concentration Measurements: NO γ-Bands as an Example." AEDC-TR-74-124 (ADA004105), January 1975.

11. Davis, M. G., McGregor, W. K., Few, J. D., and Glassman, H. N. "Transmission of Doppler Broadened Resonance Radiation through Absorbing Media with Combined Doppler and Pressure Broadening (Nitric Oxide γ-Bands as an Example)." AEDC-TR-76-12 (ADA021061), February 1976.

12. Davis, M. G., McGregor, W. K., and Few, J. D. Utilizing the Resonance Line Absorption Technique to Determine the Collisional Broadening Parameters of a Diatomic Molecule: NO γ-Bands as an Example." Journal of Quantitative Spectroscopy and Radiative Transfer, Vol. 16, No. 12, December 1976, pp. 1109-1118.

NOMENCLATURE

A_j	Area of jet exhaust plume
a	Speed of sound
a'	Line-broadening parameter, = 1,200 (±200) p/T_a
C_s	Ratio of mass of specie of interest to total mass of stream
F_i	Rotational energy of the ground state, cm^{-1}
f/a	Fuel-to-air ratio
I°_ν	Source radiation
$I^{\circ\circ}_{\nu_j}$	Intensity of the j^{th} source line at center frequency ν°_j
$k_{\nu^\circ_i}$	Doppler absorption coefficient of the i^{th} absorption line at line center frequency ν°_i
ℓ	Path length
$\Delta\ell$	Increment of path length
M	Mach number
$\dot{m}_s$	Mass flux
$\dot{m}_f$	Mass flux (fuel)
N	NO number density
Pa	Pascal, unit of measurement for pressure; 101.325 kPa = 1 atm = 14.7 psia
P_c	Test section pressure
P_j	Static pressure of exhaust stream
P_o	Static pressure of secondary stream
p	Static pressure
R	Gas constant

R_n Exhaust jet nozzle radius

r Radial distance from jet axis in the exhaust plume

S_i Rotational line strength factor (Honl-London factor)

T_a Static temperature of exhaust stream

T_T Total temperature of exhaust stream

t Transmissivity

$t_{\Delta\nu}$ Transmissivity in a given interval $\Delta\nu$ of gas of path length ℓ, containing a density N

u Velocity

y Dummy variable of integration

$(\Delta_a \nu_j)_D$ Doppler width at 1/2 $I^{\circ}_{\nu^{\circ}_j}$ of the j^{th} source line

$(\Delta_s \nu_j)_D$ Doppler width at 1/2 $k_{\nu^{\circ}_j}$ of the j^{th} absorption line

ν Frequency variable

$\Delta\nu$ Frequency interval

ρ Mass density of gas

ω_i Doppler frequency function for the i^{th} line

SUBSCRIPTS

j j^{th} line, Eq. (1)

m Reference to m^{th} zone